Mem. S.A.It. Vol. 76, 39

Memorie della

Near-infrared interferometry of AGN ⋆

G. Weigelt[1], T. Beckert[1], K.-H. Hofmann[1] D. Schertl[1], and M. Wittkowski[2]

[1] Max-Planck-Institut für Radioastronomie, Auf dem Hügel 69, 53121 Bonn, Germany e-mail: pm@mpifr-bonn.mpg.de

[2] European Southern Observatory, Karl-Schwarzschild-Str. 2, 85748 Garching bei München, Germany

Abstract. Interferometry in the infrared is able to resolve the sub-parsec-scale dust environment surrounding the accretion disk of AGN. A diffraction-limited K'-band image of NGC 1068 with 74 mas resolution and the first H-band image with 57 mas resolution were reconstructed from speckle interferograms obtained with the SAO 6 m telescope. The resolved structure consists of a compact core and an extended northern and south-eastern component. The compact core has a north-western, tail-shaped extension. The K'-band FWHM diameter of this compact core is approximately 18×39 mas ($\pm$ 4 mas) or 1.3×2.8 pc, and the position angle (PA) of the north-western extension is –16°. The PA of –16° is similar to that of the western wall of the ionization cone. This suggests that the H- and K'-band emission from the compact core is both thermal emission and scattered light from dust near the western wall of a low-density, conical outflow cavity or from the innermost region of a parsec-scale dusty torus. The first K-band long-baseline interferometry of the nucleus of NGC 1068 with resolution $\lambda/B \sim 10$ mas was obtained with the ESO VLTI. A squared visibility amplitude of 16 ± 4 % was measured at a baseline of 46 m. Taking into account K-band speckle interferometry observations, the VLTI observations suggest a multi-component structure, where part of the flux originates from scales clearly smaller than ~ 5 mas or 0.4 pc.

Key words. AGN – NGC 1068 – torus – interferometry – infrared

1. Bispectrum speckle interferometry of the Seyfert 2 galaxy NGC 1068

Diffraction-limited K-, K'-, and H-band images with 76, 74, and 57 mas resolution, respectively, (see Fig. 1) were reconstructed from speckle interferograms obtained with the SAO 6 m telescope using bispectrum speckle interferometry (Wittkowski et al. 1998; Weigelt et al. 2004). The resolved structure consists of a compact core and an extended northern and south-eastern component. The compact core has a north-western, tail-shaped extension. The K'-band FWHM diameter of this resolved compact core is $\sim 18 \times 39$ mas or 1.3×2.8 pc. The size of this resolved core was derived by fitting an elliptical Gaussian brightness distribution to the visibility functions. The position angle of the north-western extension

Send offprint requests to: G. Weigelt

⋆ Based on public commissioning data released from the VLTI and data collected at the SAO 6 m telescope in Russia.

Correspondence to: Max-Planck-Institut für Radioastronomie, Auf dem Hügel 69, 53121 Bonn, Germany

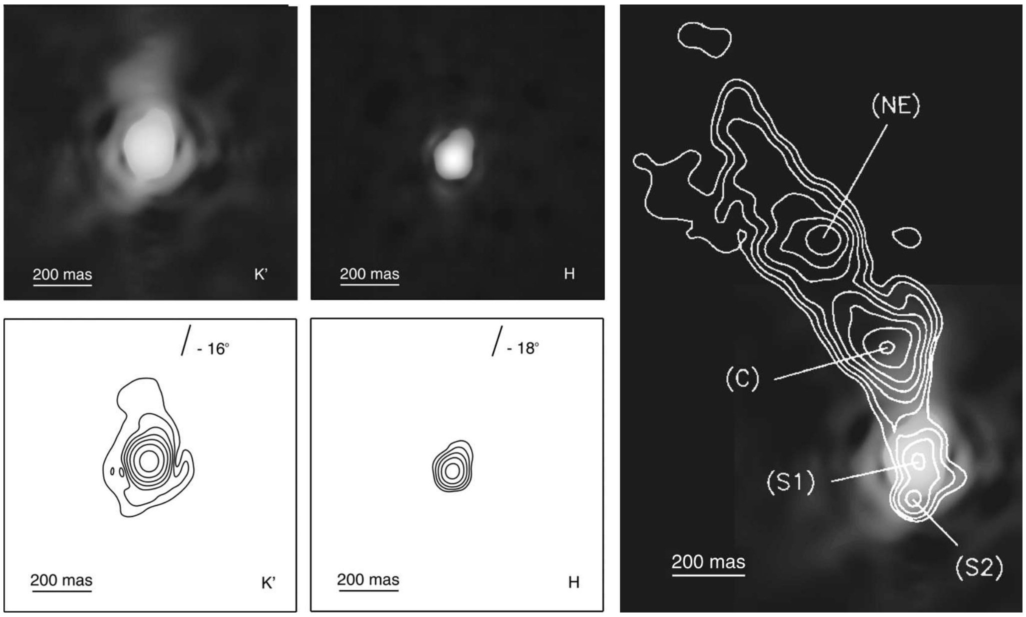

Fig. 1. Left, top, and bottom: Diffraction-limited K'-band image of NGC 1068 reconstructed by bispectrum speckle interferometry. The image shows the compact core with its tail-shaped, north-western extension at a PA of $\sim -16°$ as well as the northern and south-eastern extended components. North is up, and east is to the left. **Middle, top, and bottom:** Diffraction-limited H-band image. **Right:** MERLIN 5 GHz contour map (Gallimore et al. 1996) superposed on our K' image. The center of the radio component S1 coincides with the center of the K' peak. The PA of $-16°$ of the 18×39 mas K'-band core is very similar to that of the western wall of the ionization cone. The northern extended 400 mas structure aligns with the direction of the inner radio jet.

is $-16 \pm 4°$. The extended northern component (PA $\sim 0°$) has an elongated structure with a length of about 400 mas or 29 pc.

The PA of $-16 \pm 4°$ of the compact 18×39 mas core is very similar to that of the western wall (PA $\sim -15°$) of the ionization cone. This suggests that the H- and K'-band emission from the compact core is both thermal emission and scattered light from dust near the western wall of a conical outflow cavity or from the innermost region of a parsec-scale dusty torus (the dust sublimation radius of NGC 1068 is approximately 0.1 – 1 pc). The northern extended 400 mas structure lies near the western wall of the ionization cone and coincides with the inner radio jet. The large distance from the core suggests that the K'-band emission of the northern extended component is scattered light from the western cavity region and the radio jet region.

Emission in the K' band can be interpreted as scattered and direct thermal radiation of hot dust near its sublimation temperature. Various models have been published for NGC 1068 (e.g., Pier & Krolik 1992; Granato & Danese 1994; Nenkova et al. 2002). All these models try to fit the SED of Rieke & Low (1975) with a K-band flux of 0.3 ± 0.1 Jy. Torus models which can explain the observed infrared SED by emission exclusively from the torus were presented by Granato et al. (1997). Due to the proposed clumpiness of the torus (Krolik & Begelmann 1988; Nenkova et al. 2002; Vollmer et al. 2004) there is a possibility that a fraction of the NIR flux of the central source reaches us directly without being

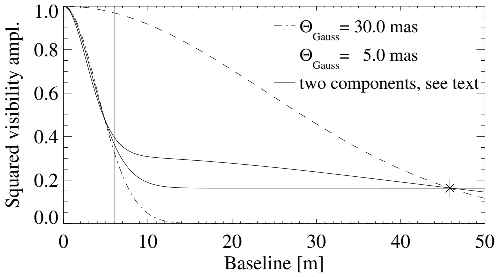

Fig. 2. Synthetic squared visibility function for a 5 mas (dashed line) Gaussian, a 30 mas (dashed-dotted line) Gaussian, and two examples (solid lines) of a two-component model where (upper line/lower line) 56%/40% of the total flux comes from a 3 mas/0.1 mas Gaussian and the remaining 44%/60% from a 54 mas/42 mas Gaussian (FWHM). Measurements are available for baselines $B = 46$ m and up to $B = 6$ m. Both measurements are only matched if the small component has a size clearly below ~ 5 mas and only if part of the total flux in our FOV arises from this small component.

strongly absorbed. Therefore, a non-negligible contribution may come from an optically thick, geometrically thin standard accretion disk surrounding the central engine or from the high-frequency tail of sychrotron emission of the radio component S1 if it is actually optically thin synchrotron radiation (Beckert & Duschl 1997; Wittkowski et al. 1998).

2. VLTI long-baseline interferometry of NGC 1068

The first near-infrared K-band long-baseline interferometry of the nucleus of NGC 1068 with resolution $\lambda/B \sim 10$ mas was obtained with the Very Large Telescope Interferometer (VLTI; two 8.2 m telescopes; Wittkowski et al. 2004). The adaptive optics system MACAO was employed to deliver wavefront-corrected beams to the K-band instrument VINCI. A squared visibility amplitude of 16.3 ± 4.3 % was measured for NGC 1068 at a sky-projected baseline length of 45.8 m (see Fig. 2). This value corresponds to a FWHM size of the observed K-band structure of 5.0 ± 0.5 mas (0.4 ± 0.04 pc) if it consists of a single Gaussian component. Taking into account K-band speckle interferometry observations (Wittkowski et al. 1998; Weinberger et al. 1999; Weigelt et al. 2004), these observations suggest a multi-component structure for the intensity distribution, where one part of the flux originates from scales clearly smaller than ~ 5 mas or 0.4 pc and another part from larger scales. The K-band emission from the small (less than 5 mas) scales might arise from the substructure of the dusty torus or directly from the central accretion flow viewed through only moderate extinction.

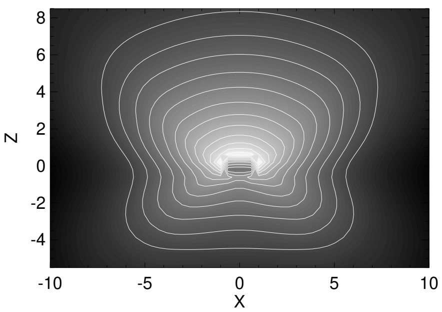

Fig. 3. K-band surface brightness of a clumpy torus model for an inclination of 60°. The dynamic range of the contour levels is 2^{12}. The linear scale of the image is in units of the dust sublimation radius. The brightest region is the illuminated inner wall on the opposite side of the torus.

3. Clumpy torus model

To explain the torus substructure in NGC 1068 mentioned above, the existence of cold and dusty clouds in a geometrically thick torus with only a few clouds along the line of sight is required. We have applied the radiative transfer treatment in a clumpy medium (Nenkova et al. 2002) to our dynamical model of clouds in the torus of NGC 1068 (Beckert & Duschl 2004). The resulting model image (Fig. 3) allows a comparison with the structures (size, shape, and flux) seen in Fig. 1.

4. Future goals

Near-infrared interferometric observations of AGN will allow us to test present unification schemes, which predict the presence of clumpy, dusty tori emitting reprocessed radiation from the NIR to the FIR. Furthermore, physical properties of outflows and jets and the connection between AGN and circumnuclear starburst activity can be studied in greater detail. These studies will improve our understanding of the fueling of black holes via accretion through nuclear disks and dusty tori. It will be possible to investigate, through a combination of interferometric observations and theoretical studies, how accretion processes at different length scales work and how they relate to each other.

The interferometric observations will show whether the theoretical torus models are viable and what kind of additional structures have to be accounted for in these models. Together with an understanding of the post-merger evolution of the large-scale ISM and associated starburst activity in the host galaxy, unique information on properties of the gas and dust available for fueling the growth of the black holes can be derived. As shown by the observations of NGC 1068, it will be possible to explore the internal structure of tori around AGN. This will provide information on dynamical processes between clouds in the torus, the resulting transport of matter, and the fueling of the black hole accretion disk. The near-infrared beam combiner instrument AMBER for the VLTI can contribute to these projects due to its high spatial resolution of 4 mas at 2 μm and 100 m baseline and its spectroscopic capabilities (spectral resolution between 30 and 10 000). The expected limiting K-band magnitude of AMBER is approximately 13 mag. AMBER will allow us to carry out phase-closure measurements with three 8 m telescopes and to reconstruct images with unprecedented angular resolution.

References

Beckert, T. & Duschl, W. J. 1997, A&A, 328, 95
Beckert, T. & Duschl, W. J. 2004, A&A, 426, 445
Gallimore, J.F., Baum, S.A., O'Dea, C.P. et al. 1996, ApJ, 464, 198
Granato, G. L. & Danese, L. 1994, MNRAS, 268, 235
Granato, G. L., Danese, L., & Franceschini, A. 1997, ApJ, 486, 147
Krolik, J. H. & Begelmann, M. C. 1988, ApJ, 329, 702
Nenkova, M., Ivezić, Ž., & Elitzur, M. 2002, ApJ, 570, L9
Pier, E. A., Antonucci, R., Hurt, T., Kriss, G., & Krolik, J. 1994, ApJ, 428, 124
Pier, E. A. & Krolik, J. H. 1992, ApJ, 401, 99
Rieke, G. H. & Low, F. J. 1975, ApJ, 199, L13
Vollmer, B., Beckert, T., & Duschl, W. J. 2004, A&A, 413, 949
Weigelt, G., Wittkowski, M., Balega, Y., et al. 2004, A&A, 425, 77
Weinberger, A. J., Neugebauer, G., & Matthews, K. 1999, AJ, 117, 2748
Wittkowski, M., Balega, Y., Beckert, T., et al. 1998, A&A, 329, L45
Wittkowski, M., Kervella, P., Arsenault, R., et al. 2004, A&A, 418, L39